PERGAMON

Journal of Structural Geology 22 (2000) 1587–1600

JOURNAL OF STRUCTURAL GEOLOGY

www.elsevier.nl/locate/jstrugeo

Lattice strain measurements on sandstones under load using neutron diffraction

A. Frischbutter[a,*], D. Neov[b], Ch. Scheffzük[a,c], M. Vrána[b], K. Walther[a]

[a]*GeoForschungsZentrum Potsdam, PB 5.3, Telegrafenberg, D-14473 Potsdam, Germany*
[b]*Nuclear Physics Institute, Czech Academy of Science, CR-25068 Řež near Prague, Czech Republic*
[c]*Frank Laboratory of Neutron Physics, Joint Institute for Nuclear Research, 141980 Dubna, Russia*

Received 17 December 1999; accepted 13 July 2000

Abstract

Neutron diffraction methods (both time-of-flight- and angle-dispersive diffraction) are applied to intracrystalline strain measurements on geological samples undergoing uniaxial increasing compressional load. The experiments were carried out on Cretaceous sandstones from the Elbezone (East Germany), consisting of >95% quartz which are bedded but without crystallographic preferred orientation of quartz. From the stress–strain relation the Young's modulus for our quartz sample was determined to be (72.2 ± 2.9) GPa using results of the neutron time-of-flight method. The influence of different kinds of bedding in sandstones (laminated and convolute bedding) could be determined. We observed differences of factor 2 (convolute bedding) and 3 (laminated bedding) for the elastic stiffness, determined with angle dispersive neutron diffraction (crystallographic strain) and with strain gauges (mechanical strain). The data indicate which geological conditions may influence the stress–strain behaviour of geological materials. The influence of bedding on the stress–strain behaviour of a laminated bedded sandstone was indicated by direct residual stress measurements using neutron time-of-flight diffraction. The measurements were carried out six days after unloading the sample. Residual strain was measured for three positions from the centre to the periphery and within two radial directions of the cylinder. We observed that residual strain changes from extension to compression in a different manner for two perpendicular directions of the bedding plane.

1. Introduction

Improved knowledge of the present stress state of the Earth's crust is required for commercial and scientific purposes. Examples include oil- and gas-exploration, civil underground mining, hazard assessment projects within the frame of environmental conservation, as well as fundamental research. The aim is a better understanding of the complicated, multifaceted processes involved in the deformation of the Earth's crust.

Estimations of the present stress state of the Earth's crust ('World Stress Map' by Zoback, 1992) are based on the maximum horizontal stress orientation, derived from earthquake data (fault plane solutions), overcoring experiments, hydraulic fracturing, borehole breakouts and geological data such as fault slip data and volcanic alignments. Recently, an attempt was made to derive the present stress pattern for the East European Platform from remote sensing data (Sim et al., 1999). The traditionally geodetic method of triangulation was recently replaced by measurements from satellites (the GPS-technique). A comprehensive review of stress related to the Earth, including methods of stress determination in geosciences was given recently by Amadei and Stephansson (1997).

All of the methods of stress-assessment obtain a projection of associated strain values into a horizontal plane and give no quantitative information. Moreover, they do not consider structural influences such as macro- (e.g. bedding, faulting etc.) and/or microstructures (e.g. texture in the sense of crystallographic preferred orientation) or the role of residual stresses in rocks. The consequences of the latter are of great technical importance in material sciences (Hutchings, 1992) but are also well known in field geology in the form of rockbursting, rock surface spalling, core discing etc. Residual stresses are present in rocks which have been subject to high pressure and/or temperature (Voight, 1966). They represent a self equilibrating energy level, which remains even after unloading, expansion, cooling or uplifting, drilling or sampling. Moreover, on investigating multiphased systems like rocks consisting of minerals with different thermoelastic properties we can obtain information on paleostresses as an estimation of the maximum value for geological determined events. The

* Corresponding author. Fax: +49-331-288-1127.
E-mail address: fribu@gfz-potsdam.de

0191-8141/00/$ - see front matter
PII: S0191-8141(00)00110-3

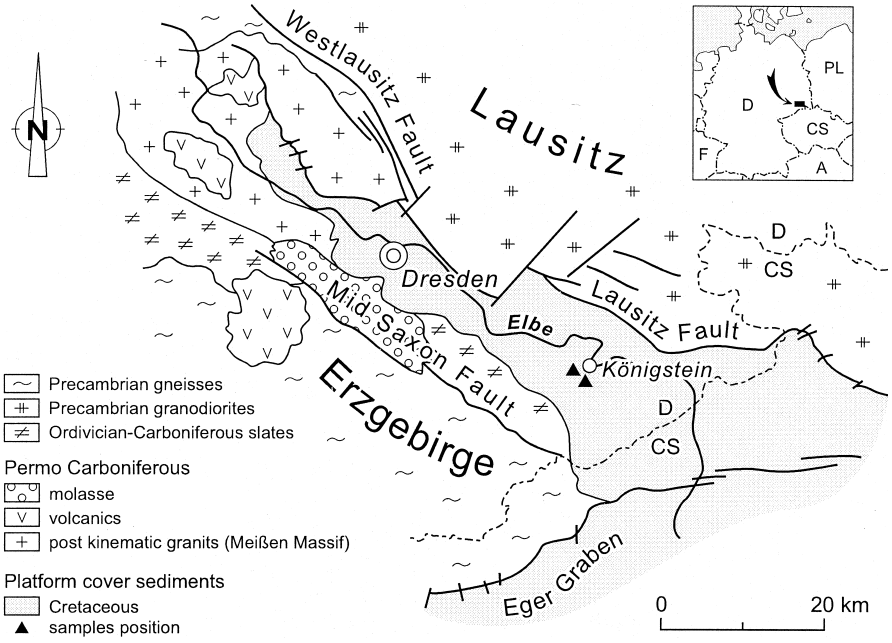

Fig. 1. Geological sketch of the Elbezone between Erzgebirge and Lausitz.

residual stresses in rocks and especially their influence on the behaviour of repeatedly deformed rocks have rarely been studied by geoscientists until now or are a matter of controversial discussion.

In this work the authors introduce a method of intracrystalline strain measurement using diffraction methods. X-ray and neutron diffraction have been long time successfully applied in material sciences (metals, ceramics) to estimate residual stress states or to study experimentally defined loading conditions within a workpiece. The state-of-the-art of strain measurements using diffraction methods in the material sciences was presented for instance by Eigenmann and Macherauch (1995). However, up to now there are only a few published papers dealing with strain measurements on geological samples using X-ray diffraction (Friedman, 1972; Reik, 1976). The reason for the rather restricted success of those studies was the low penetration depth of X-rays (within the order of 0.01 mm), which causes distinct surface and grain size effects. A new situation arose when geologists started to use neutron diffraction for experiments on geological samples, because the high penetration depth of neutrons allowed sample volumes of several cm^3 to be studied. Neutron diffraction has been successfully applied to texture investigations on rocks consisting of low symmetric crystals since the middle of the eighties (e.g. Wenk, 1981; Wenk, 1985; Bankwitz et al., 1985). Efforts have been made recently to apply the method to stress–strain estimations on geological samples. The first results of direct intracrystalline strain measurements using angle-dispersive and time-of-flight neutron diffraction have been published by Scheffzük et al. (1998a,b) and Walther et al. (1998). Time-of-flight neutron diffraction is an especially advantageous method for geological materials because all permitted Bragg-reflections can be determined simultaneously. A 'white' or polychromatic neutron beam (which has a wideband neutron spectrum) allows the simultaneous observation of multiple lattice spacings. This, and the fact that no angle correction is needed, increase the accuracy of the measurement and is especially helpful for the investigation of minerals with lower crystal symmetry (large unit cell), of which the upper Earth's crust mainly consists.

Diffraction methods aim to measure the change of the lattice spacings due to deformation directly. First order- or macro-stress is documented by a change of the peak position and second order stress is expressed by peak broadening (related to dislocation densities). The main advantages of diffraction experiments are the possibility of studying the deformation behaviour of lattice spacings under changing load conditions in sample volumes of several cm^3 and the possibility of quantitative determination of the complete strain tensor.

This paper summarizes results of strain measurements on natural sandstone undergoing different load conditions, using both time-of-flight and angle-dispersive (conventional) neutron diffraction and discusses results of residual stress measurements on experimentally deformed rocks. The experiments were carried out at the steady state reactor of the Czech Academy of Science in Řež (Czech Republic) and at the pulsed reactor IBR-2 of the Joint Institute for Nuclear Research (JINR) in Dubna (Russia).

2. Geological background

The specimens were prepared from cores of ground water holes in the Elbezone, drilled close to Königstein (Fig. 1), a

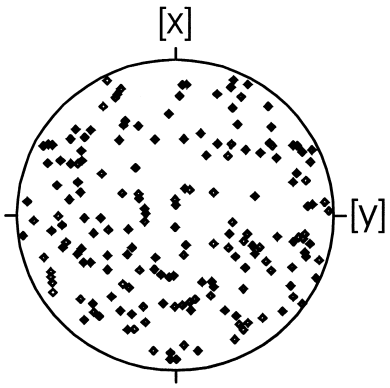

Fig. 2. Distribution pattern of 200 quartz [*c*]-axes of the studied sandstone, measured on the universal stage and related to the bedding plane (equal area projection, lower hemisphere).

town about 20 km SE of Dresden (East Germany). The Elbezone represents a first order structural element of the Earth's crust trending parallel to the SW-border of the East European Platform. The structure was first active at about 600 Ma ago and then subjected to repeated episodes of crustal reactivation. The Elbezone separates Precambrian crust units of extremely different geological evolution, such as the high-grade gneisses of the Erzgebirge and the anatectic granodiorites of Lausitz. An asymmetric half graben was formed following the Elbezone mainly during Cretaceaous times. The graben (intersected near Dečin by the NE–SW-trending Eger Graben of Tertiary age) is connected to the SE with the Bohemian Cretaceous and mainly filled with marine, clastic sediments (sandstones). Since the Upper-Cretaceous, the graben has been closed and overthrusted partly along the 30° NE-dipping Lausitz Störung by the Lausitz granodiorites (Müller and Wächter, 1970). Strike-slip movements possibly occurred along the NW-trending border-faults of the Elbezone. Similar to its NE-border, the SW-limitation of the Elbezone (Mittelsächsische Störung) is characterized by SW-vergent overthrusting. Younger Paleozoic units of the Elbezone are found on the Precambrian Erzgebirge gneisses. Additionally, oblique dextral shearing was observed (Rauche, 1992). Finally, the Elbezone is characterized by weak recent activity. Interpretations of repeated geodetic triangulations (Thurm et al., 1968, 1977) show that the Elbezone is recently a 10–25 km wide NW–SE-trending zone, characterized by NE–SW-directed extension, by small zones of compression and cut by predominantly N–S directed sinistral shear zones.

Quartz is one of the best known and most frequently occurring minerals in the upper continental crust and occurs in a range of geological conditions, e.g. in relation to other associated minerals or to different macro-structure (grain size, bedding, schistosity), micro-structure (crystallographic preferred orientation, dislocation density) or deformation history (metamorphism and un- up to poly-deformed). From the mechanical point of view and compared to other important rock forming minerals quartz reacts brittle under the conditions of the uppermost crust. From this arises a good contrast, e.g. in relation to much more ductile minerals like mica or calcite. We therefore think that quartz is suitable for first experiments adapting neutron diffraction methods for geological problems.

The Cretaceous sandstones of the Elbezone were selected because they are undeformed, quasi-monomineralic in composition and available with different types of bedding. Samples were taken from cores of ground water holes (HG 7012) at a drilling depth of approximately 250 m below surface level. The cores were taken without orientation marks, thus the coordinate system could be fixed only in relation to the bedding plane: (*xy*) within the bedding and [*z*] perpendicular to the bedding plane and fixed by the core bit. From the original cores with a diameter of 100 mm cylinder-specimens were prepared with the following diameter/length relations: e.g. 30 mm/60 mm, 20 mm/40 mm and in single cases 40 mm/100 mm.

The average composition of the sandstone is 95% quartz with minor concentrations of accessories (5%) such as potassium-feldspar, white mica, calcite, dolomite (determined by quantitative X-ray-phase analysis). The grain size varies in the range from 100 to 200 μm. Occasionally rock fragments occur (mainly of granitic composition) which may be up to 1 mm in diameter. Quartz is mostly clastic and equigranular. The grains are only weakly rounded. Microscopic observations show that some quartz grains (mostly within rock fragments) have undulatory extinction, which is explained as a feature inherited from the parent rock and not due to a post-Cretaceous deformation event. The pore volume of the rocks is in the order of 10%.

The sandstone is characterized by absence of crystallographic preferred orientation of quartz grains. Fig. 2 shows the distribution pattern of 200 quartz [*c*]-axes, measured on the universal stage. Sandstones have well-developed bedding of different qualities. Two types of bedding were examined. One sample represents a laminated, planar formed bedding, characterized by variable grain size (representing anisotropic conditions); the other type shows uneven bedding planes (convolute), and is characterized by inclusions of fossil shells and/or synsedimentary redeposition (representing more or less isotropic conditions).

3. Neutron time-of-flight (polychromatic) diffraction

The basis for diffraction methods is Bragg's law: $\lambda = 2d_{hkl}\sin\vartheta$ where λ is the wavelength, d_{hkl} is the lattice plane spacing and ϑ is the Bragg angle.

In contrast to the conventional diffraction technique steady state reactors, where a monochromated neutron beam is used, the time-of-flight (TOF) method needs a 'white' neutron beam. The kinetic energy of the neutrons is estimated in the frame of classical mechanics. The time is

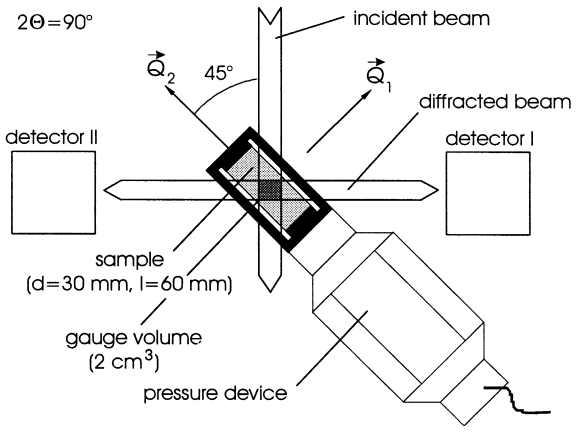

Fig. 3. Layout of the neutron time-of-flight diffractometer Epsilon at the reactor IBR-2 at the beam line 7A. $\vec{Q}_1$ and $\vec{Q}_2$ are the scattering vectors.

measured which the neutrons need for passing the path from the reactor (surface of the moderator) via the sample to the detector. As an object of quantum physics, neutrons exhibit both particle and wave properties. A particle property, e.g. velocity or momentum, corresponds to a certain wave property such as wavelength. The wavelength is directly proportional to the time needed for the flight through the known flight path, i.e. neutrons with short wavelengths are recorded by the detector earlier than neutrons with large wavelengths. In order to get a fixed assignment between the TOF and the velocity or wavelength of the neutrons all neutrons must commence their flight within a small time interval, i.e. the neutron source must be a pulsed one. For all TOF-experiments we use the pulsed neutron source IBR-2 at the Joint Institute for Nuclear Research in Dubna (Russia).

3.1. Experimental procedure

Strain measurements were performed on the Epsilon neutron diffractometer which is situated about 102 m away from the surface of the moderator. The neutrons (natural isotopic abundance) are guided to the sample by a Ni-coated straight neutron guide. The neutron guide starts in the biological shield (approximately 8 m from the moderator surface); the first 18 m of the neutron guide is filled with Ar, the far part of the guide is evacuated. The reactor functions with a pulse repetition rate of 5 Hz. The mean power of the reactor is about 1.5 MW; the power at the moment of the neutron burst is about 1200 MW. Between two pulses the reactor works like a steady state 100 kW reactor. An additional chopper situated about 6 m away from the surface of the moderator reduces the noise of the neutron radiation between the pulses.

The mean flux at the surface of the moderator is about 6×10^{12} n cm^{-2} s^{-1}, the flux at the sample is about 0.75×10^{6} n cm^{-2} s^{-1}. The duration of the thermal neutron pulse is about 320 μs. The moderator has a 'grooved' shape and is filled with light water.

Due to the long flight path, a good spectral resolution $\Delta d/d = \Delta t/t$ of 4×10^{-3} (for a lattice spacing $d > 0.2$ nm) is achieved where Δd and Δt are the full width at half maximum of the diffraction peak in units of the lattice spacing and time respectively. These conditions permit the measurement of samples consisting of lower symmetry crystals (even mica and feldspar).

The sample is mounted either inside a pressure device or on a goniometer head. Two detectors are set up with a scattering angle of $2\vartheta = \pm 90°$; thus one detector is able to measure the diffraction pattern in the direction of the applied load, the other one in the direction perpendicular to the load (Fig. 3).

The diffractometer Epsilon is equipped with a pressure device (Exstress). This device provides an uniaxial load of maximal 100 kN which corresponds to a maximal stress of 150 MPa for cylindrical samples with dimensions of 30 mm in diameter and 60 mm length. An AC-motor is coupled to a planet gear-box and drives a screw shaft, which acts on the moveable head of the press. Between the head and the base surface plane of the sample a gauge for measuring the force is situated. The AC-motor can be controlled with respect to the torque (i.e. the force), velocity and number of rotations (steps) of the shaft. The force F, the displacement Δl of the head of the press and the ambient temperature T are measured online. The sample is not confined in a jacket or other medium. In general, the sample is loaded until failure.

At first the diffraction pattern is measured for the unloaded state of the sample. The load is subsequently increased in almost equidistant steps. The measurement of each step takes about 24 h. As mentioned above, the time axis of the diffraction pattern corresponds to the wavelength of the diffracted neutrons or to the lattice spacing of the sample. The channel width of time channels of the multichannel time-analyser is chosen to be 32 μs and the maximum number of time channels provided by the time analyser is 4096. Fig. 4 shows the time-of-flight diffraction pattern of a sandstone sample. Due to the asymmetry of the neutron pulse the peak shape of the diffraction pattern is also asymmetric. We describe the peak shape as a combination of two (half) Gaussians, one for the left side of the peak and the other one for the right side. Therefore we obtain two half-widths. The mathematical expression of the peak shape is

$$f(x) = a_0 \begin{cases} e^{-\left(\frac{x-x_0}{2\sigma_l}\right)^2} & x < x_0 \\ e^{-\left(\frac{x-x_0}{2\sigma_r}\right)^2} & x \geq x_0 \end{cases}$$

where a_0 is the peak amplitude, x_0 is the centre of the peak, and σ_l and σ_r are the width parameters.

The lattice deformation ε is described by the relative distance variation of lattice planes between the stress-free state and the state undergoing stress, d^0_{hkl} and d_{hkl}, respectively, or the times of flight t_{hkl} for the diffraction peak under

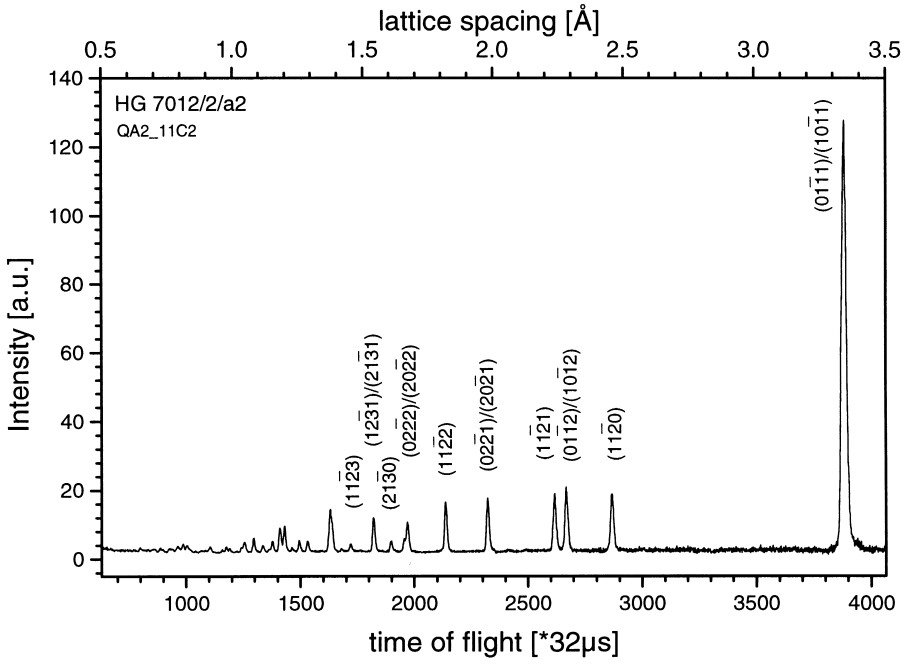

Fig. 4. TOF diffraction pattern of a sandstone measured at the diffractometer Epsilon. Some of the quartz peaks are indexed.

investigation and t^0_{hkl} for the unloaded sample (both t_{hkl} and t^0_{hkl} are the centres of the Gaussian peaks, measured in units of time):

$$\varepsilon_{hkl} = \frac{d_{hkl} - d^0_{hkl}}{d^0_{hkl}} = \frac{t_{hkl} - t^0_{hkl}}{t^0_{hkl}}$$

If the strain within the gauge volume is homogeneous, i.e. strain of type I, the peak is shifted along the time axis of the diffraction pattern. Comprehensive strain causes a peakshift toward lower time values and extensional strain in the opposite direction. The peak centres are resolved to at least two decimal places using peak-fit programs. The accuracy of the estimation of the centre of the peak depends on the statistical error of the diffraction pattern. Usually the fit error of the peak position is of the order of 0.02 time channels. Thus the strain is measured to better than 10^{-5}. The peaks are fitted separately. The background correction is also done separately for each peak. Prior to the peak fitting procedure the diffraction pattern is corrected for the wavelength-distribution of the source by dividing the recorded pattern by the pattern taken with a Vanadium-standard sample (i.e. the so called reactor spectrum).

A central problem of strain measurement is the estimation of the lattice spacing d_0 for the unloaded sample. If an equivalent material of the same composition is available, a powder etalon of the material under investigation is usually prepared. In other cases, where powder of the same composition or strain-free etalons are not available, alternative methods for the d_0-estimation are proposed. In the case of X-ray diffraction, where the penetration of X-rays can be neglected, it is assumed that the component ε_z perpendicular to the surface will vanish and therefore the $d(\psi)$ value for the tilt angle $\psi = 0$ is assumed to be the d_0-value. Wieder (1996) proposed that the unknown d_0-values be calculated together with the values for the stress and the strain with a least-squares fit. This method works for all crystal symmetries and is not limited to special stress states. The number of free parameters is 13 for cubic crystal symmetry; for lower crystal symmetry even more.

In preparing a powder etalon, the process of grinding may itself be a source of (micro)stresses. The powder is annealed particularly in experiments with iron and other metallic samples, because the stresses should vanish due to annealing (soft annealing). For our geological experiments we determined d_0 for powders, made from identical specimens, ground up to a grain size less than 62 μm, homogenized, heated to 500°C over 24 h and finally cooled within the closed stove. These annealed powders and the original ones are used for the measurement of d_0. In Fig. 5 the position of six peaks are shown; their peak-widths (full width at half maximum, FWHM) are given as error bars. There are small differences in statistical errors for the investigated powders, but independent of the heat treatment. The statistical errors strongly depend on the intensity of the Bragg reflection, so that the lowest statistical errors are observed for the $(01\bar{1}1)/(10\bar{1}1)$ peak. Both the different samples and the different annealing conditions are given. The relative deviation for all data varies between 0.05×10^{-4} and 0.8×10^{-4}. Nevertheless, those studies are measuring time consuming, but they are necessary to improve our knowledge of possible differences in the characteristics of a given lattice plane.

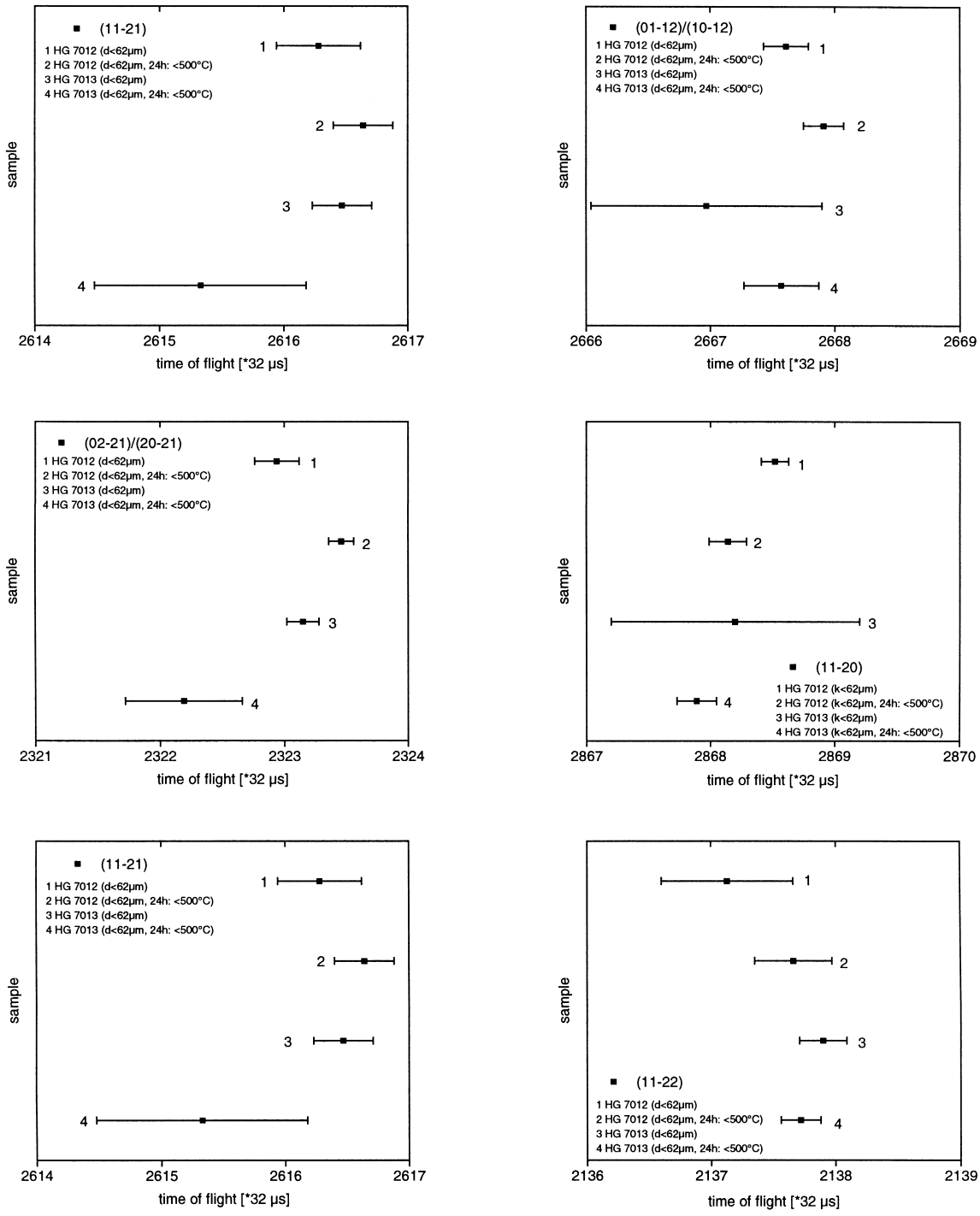

Fig. 5. Positions of some quartz peaks determined on two powder samples (1/2 and 3/4), each only grinded (1 and 3) and additionally heat- treated for 24 h at 500°C (2 and 4).

3.2. Results

In Figs. 6–8 the position of the $(01\bar{1}1)/(10\bar{1}1)$, $(11\bar{2}0)$ and $(01\bar{1}2)/(10\bar{1}2)$ quartz peaks are shown as a function of the applied stress. The results reflect a linear peak shift depending on the increasing applied load. The linear dependence of the measured strain on the applied stress demonstrates the elastic behaviour of the rock's material, so that the observed lattice contractions are consistent with the Hooke's law. The Young's moduli were determined for the lattice planes $(01\bar{1}1)/(10\bar{1}1)$, $(11\bar{2}0)$ and $(01\bar{1}2)/(10\bar{1}2)$ by linear fitting. They are listed in Table 1 against the 'theoretical' values. The 'theoretical' values are values of the Young's modulus of a single crystal for the given crystallographic direction. They are only illustrative in this context and have no meaning for the discussion of the results. The obtained Young's

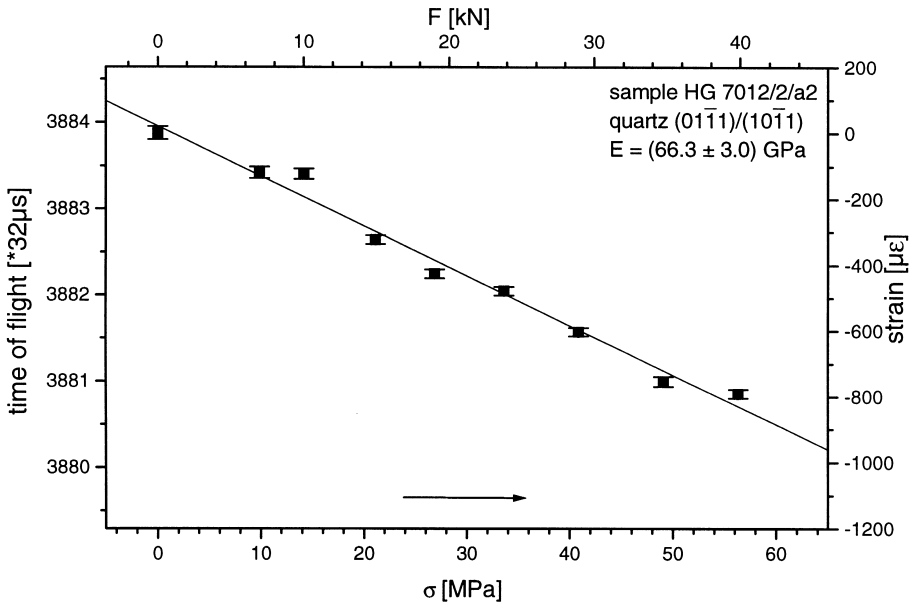

Fig. 6. Deformation of the quartz sample HG 7012/2/a2 due to the uniaxial load up to 56.33 MPa. It is shown the shift of the (01$\bar{1}$1)/(10$\bar{1}$1) peak. The strain was observed by neutron TOF diffraction. The Young's modulus was determined by linear regression to $E = (66.2 \pm 3.0)$ GPa.

moduli are in all cases smaller than the 'theoretical' ones, due to expected effects from grain boundaries, accessory phases, pore volume and texture amongst others.

Furthermore, in addition to peak shift, peak broadening was observed, which is an indicator of increased second order stresses. Fig. 9 shows the dependence of the peak width (FWHM) of the (11$\bar{2}$0) Bragg reflection on the applied load. Neglecting the runaway FWHM-value at $\sigma = 40.8$ MPa, a relationship between FWHM and the stress σ was determined by linear regression to be $(2.4 \pm 1.3) \times 10^{-2}$ time channels per MPa.

3.3. Residual strain

Residual strain (RS) was measured spatially resolved at the same sample six days after unloading. The time difference between applied load and residual strain measurements was determined by the reactor time schedule. We observed three positions within different depths in radial directions from the centre to the surface of the sandstone cylinder, following profiles arranged in the directions [x] and [y], which are mutually perpendicular and determine the bedding plane of the sandstone. An identical gauge volume

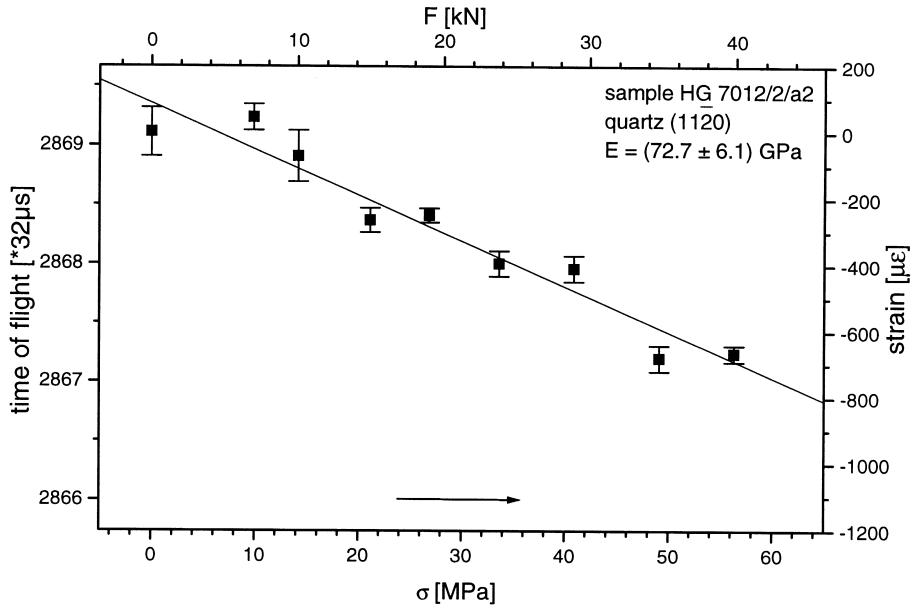

Fig. 7. Deformation of the quartz sample HG 7012/2/a2 due to the uniaxial load up to 56.33 MPa. It is shown the shift of the (11$\bar{2}$0) peak. The strain was observed by neutron TOF diffraction. The Young's modulus was determined by linear regression to $E = (72.7 \pm 6.1)$ GPa.

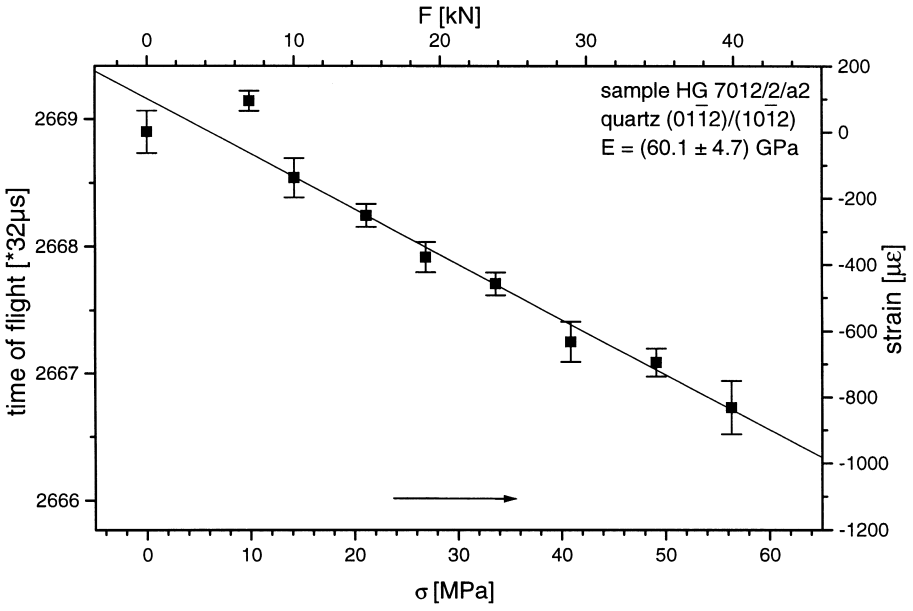

Fig. 8. Deformation of the quartz sample HG 7012/2/a2 due to the uniaxial load up to 56.33 MPa. It is shown the shift of the (01$\bar{1}$2)/(10$\bar{1}$2) peak. The strain was observed by neutron TOF diffraction. The Young's modulus was determined by linear regression to $E = (60.1 \pm 4.7)$ GPa.

for each position was realized using the translation stages of the EPSILON diffractometer. All recorded volumes were located completely within the sample.

It is noteworthy that the results indicate an anisotropy of residual strain distributions within the bedding plane. In Fig. 10, the residual strain is shown for the strongest Bragg reflections (01$\bar{1}$1)/(10$\bar{1}$1), (11$\bar{2}$0) and (01$\bar{1}$2)/(10$\bar{1}$2) in [x] and [y]-direction. For the [x]-direction, the centre of the sample shows extensional RS and at the margin compressional RS. For the [y]-direction, the residual strain develops in the opposite sense.

4. Angle-dispersive (monochromatic) neutron diffraction

4.1. Experimental procedure

The neutron diffraction experiments using monochromatic neutron radiation were carried out at the research reactor LVR-15 (light water cooled, light water moderated) at the Nuclear Physics Institute of the Czech Academy of Sciences in Rez, near Prague (Vrána et al., 1994; Mikula et al., 1997). The analyser and the original detector unit of the triple-axis

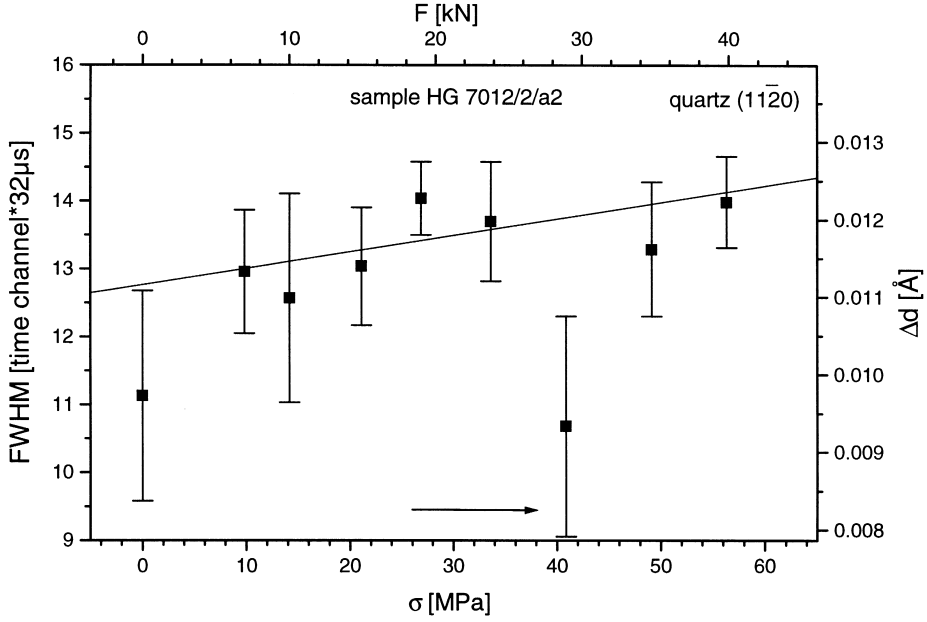

Fig. 9. Deformation of the quartz sample HG 7012/2/a2 due to an applied uniaxial load up to 56.33 MPa. It is shown the peak broadening as full width at the half maximum (FWHM) of the (11$\bar{2}$0) reflection. The peak broadening was determined by linear regression to be $(2.4 \pm 1.3) \times 10^{-2}$ time channels per MPa.

Table 1
The obtained Young's moduli of the lattice planes $(01\bar{1}1)$, $(11\bar{2}0)$ and $(01\bar{1}2)$

	The Young's moduli	
Lattice plane	Determined (GPa)	Theoretical (GPa)
$(01\bar{1}1)/(10\bar{1}1)$	66.2 ± 3.0	83.9
$(11\bar{2}0)$	72.7 ± 6.1	78.1
$(01\bar{1}2)/(10\bar{1}2)$	60.1 ± 4.7	91.6

spectrometer TKSN-400 were replaced by a linear position-sensitive detector (PSD) which covers a 2ϑ-range of about 7 degrees and works in the diffractometer mode. The spectral resolution $\Delta d/d$ is about 0.2%.

In a special regime a bent Si-monochromator is used as monochromator. Using the (220)-reflection ($\lambda = 0.23$ nm) the bent monochromator provides a very good resolution for a small region in the 2ϑ-range (2ϑ about 80°). The $(02\bar{2}1)/(20\bar{2}1)$-reflection of quartz is inside this region and is therefore chosen for the strain measurements.

The diffractometer for strain measurements is equipped with a deformation device for both tension and compression. The maximum load is 55 kN, the typical movement of the piston is about 12–24 μm for each measuring step. The elapsed time for one measurement is about 4000–12 000 s. The press operates with equidistant steps of the piston. The

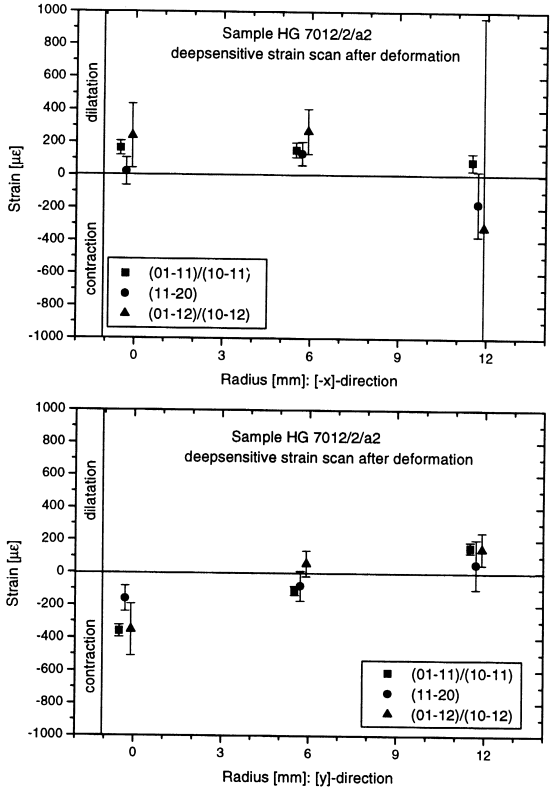

Fig. 10. Determination of the residual strain in [x]- and [y]-direction by scanning in radial direction. The xy-plane is the bedding plane. The strain was measured six days after unloading.

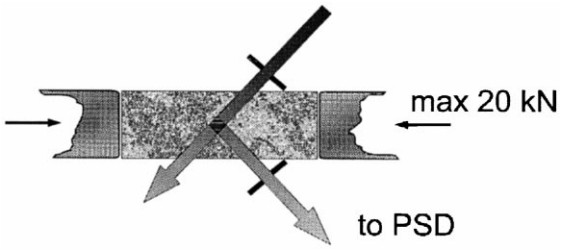

Fig. 11. Scattering geometry for the angle-dispersive experiments on sandstones under load. The gauge volume is determined by slits of 2 mm width and 30 mm height.

movement of the piston (i.e. macrostrain of the sample) is controlled both by a rotational sensor at the screw shaft and by strain gauges glued at the sample. The lattice strain ε_{hkl}, i.e. the microscopic strain, is calculated from the observed displacement $\Delta\vartheta_{hkl}$ of the maximum of the diffraction peak: $\varepsilon_{hkl} = \dfrac{(d_{hkl} - d^0_{hkl})}{d^0_{hkl}} = -\cot\vartheta_{hkl}\Delta\vartheta_{hkl}$ where ϑ_{hkl} is the Bragg angle, d_{hkl} is the measured lattice spacing and d^0_{hkl} is the lattice spacing without load. The last was estimated by measurement of powder.

Six cylindrical specimens (20 mm diameter, 40 mm length) were prepared from sandstones of two different types of bedding (laminated and convolute), with their axes in three mutually perpendicular directions, i.e. orientated in relation to the bedding plane (ss) and the core bit. The specimens were fixed horizontally within the deformation device by using cylindrical mountings of 20 mm in diameter but without any confinement medium or jacket. Both incident and diffracted beam were limited by a diaphragm with slits of 2 mm width and 30 mm height, which determine the gauge volume (Fig. 11).

4.2. Results

Prior to the loading experiments, the composition of the studied samples was checked by the diffraction measurement over an extended 2ϑ-range. The obtained diffraction pattern (Fig. 12) confirms the phase composition, as determined by quantitative X-ray analysis and point counting under the microscope (>95% quartz). A similar spectrum was recorded at the neutron TOF diffractometer EPSILON (Fig. 4) in Dubna on an equivalent specimen prepared from the same core.

The high instrumental resolution in this experiment enable the measurement of even small peak shifts during the deformation experiment (Vrána et al., 1994). However, even in this case good statistics was proven to be a crucial point to the measurements. The results are shown in Fig. 13(a-f). For each sample the curve for the intracrystalline strain, measured by diffraction and for the sample-strain simultaneously measured with a strain gauge are given. Sample 3b/1 (Fig. 13e) failed already at a load of ca. 20 MPa, probably due to inhomogeneous deformation. The somewhat earlier failure of sample 1c/1 (Fig. 13a) may

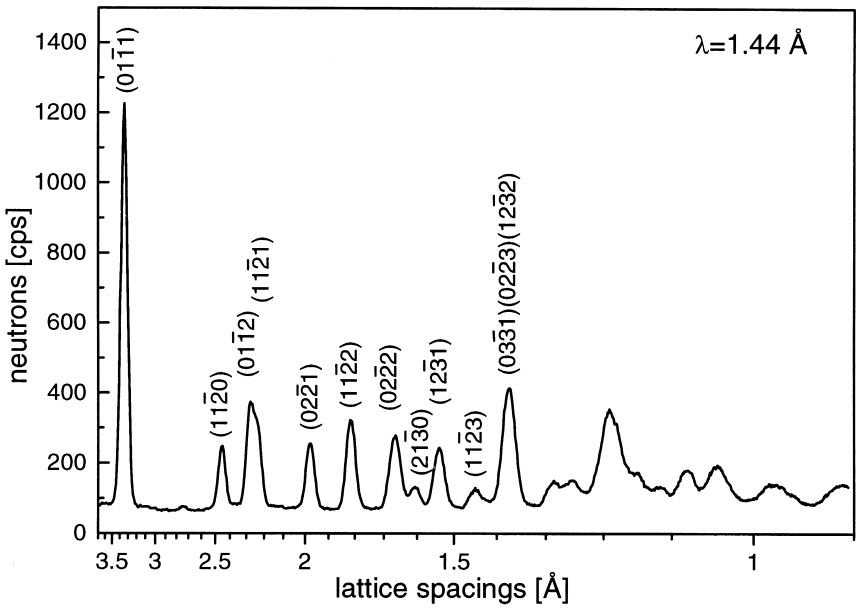

Fig. 12. Angle-dispersive neutron diffraction pattern of the tested sandstones.

have been caused by the sample orientation to bedding and/or by other structures of earlier deformations. All other specimens supported the maximum possible applied stress of approximately 55 MPa. After unloading only single small cracks could be observed.

From the slope of the graphs the crystallographic and mechanical elastic stiffness data were calculated assuming the validity of Hooke's law. The elastic moduli determined by the diffraction experiment do not differ very much from the crystallographic constants for the α-quartz monocrystal (Table 1). As expected there is a clear difference between the data determined crystallographically and mechanically. Additionally, the difference between crystallographically and mechanically determined values is in the order of a factor three in case of the laminated bedded sandstones but less than two for the convolute bedded samples (Table 2). The strain determined from the strain gauge must be regarded to be smaller than or even equal to the true deformation of the sample. Apart from the results for sample 3b/1 (Fig. 13e) which may be influenced by inhomogeneous deformation we obtain a higher degree of similarity to the mechanically determined strain data for all experiments (laminated and convolute bedding) but a more distinct difference between the data for laminated and convolute bedded sandstones regarding the crystallographic values.

5. Discussion

Stress/strain observation on geological samples using neutron diffraction is still not a completely developed method. Apart from a drastic reduction of the measuring time presently needed for the determination of a strain tensor, more measurements are required to determine and evaluate possible sources of error. In order to obtain precise reference values for d_0 it is necessary to measure a reference sample under the same geometrical conditions as the samples under investigation. A consistent geometry is important because different gauge volumes or different gauge volume geometries will lead to geometrical errors such as nonidentical beam paths and different resultant absorption and attenuation. Furthermore, multiple scattering and wavelength-dependent attenuation have to be considered (Hsu et al., 1995). We prefer to prepare our reference sample from the same material which is later measured in the experiment.

Precise knowledge of the diffraction line-profile shape is of the utmost importance in strain analysis, as well as in X-ray and neutron diffraction. Taking into consideration that in our case the Bragg reflections have an asymmetrical shape, errors may occur due to poorly adapted line-profiles for peak-fitting.

One of the main advantages of the TOF diffraction is the fixed scattering geometry, i.e. there is no need for detector movements, so this can not be a source of error. The measurements in Řež are performed with 1d PSD, where the detector unit was fixed, so there are also no errors due to detector movement.

The peak position errors for TOF diffraction are given by $\frac{\Delta d_{hkl}}{d_{hkl}} = \frac{\Delta L}{L} + \frac{\Delta t}{t} + \cot\vartheta\Delta\vartheta$ where L is the total flight path, t is the time of flight and ϑ is the Bragg's angle. The time-error is mainly given by the width of the neutron pulse (approximately 320 μs, i.e. 10 times the width of one digitized time channel). The angle error is due to the transmission of the SÖLLER collimator and is 18 minutes or 0.3°. Increasing the scattering angle decreases the influence of the angle error. In the case of back scattering this term

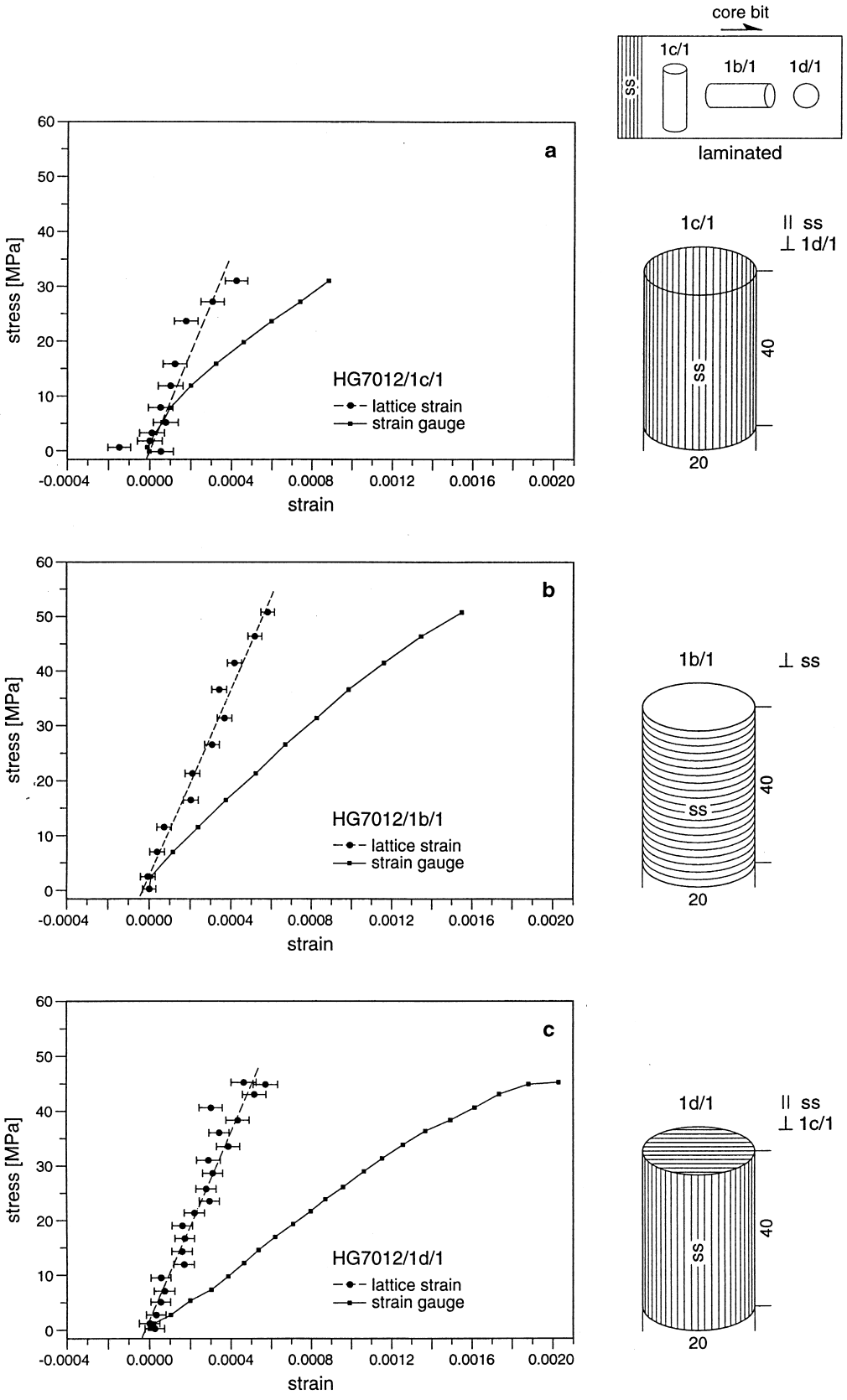

Fig. 13. Macroscopic and microscopic stress–strain curves for experiments on sandstones with laminated (a–c) and convolute bedding (d–f), determined by neutron diffraction (lattice strain) and mechanically (strain gauge).

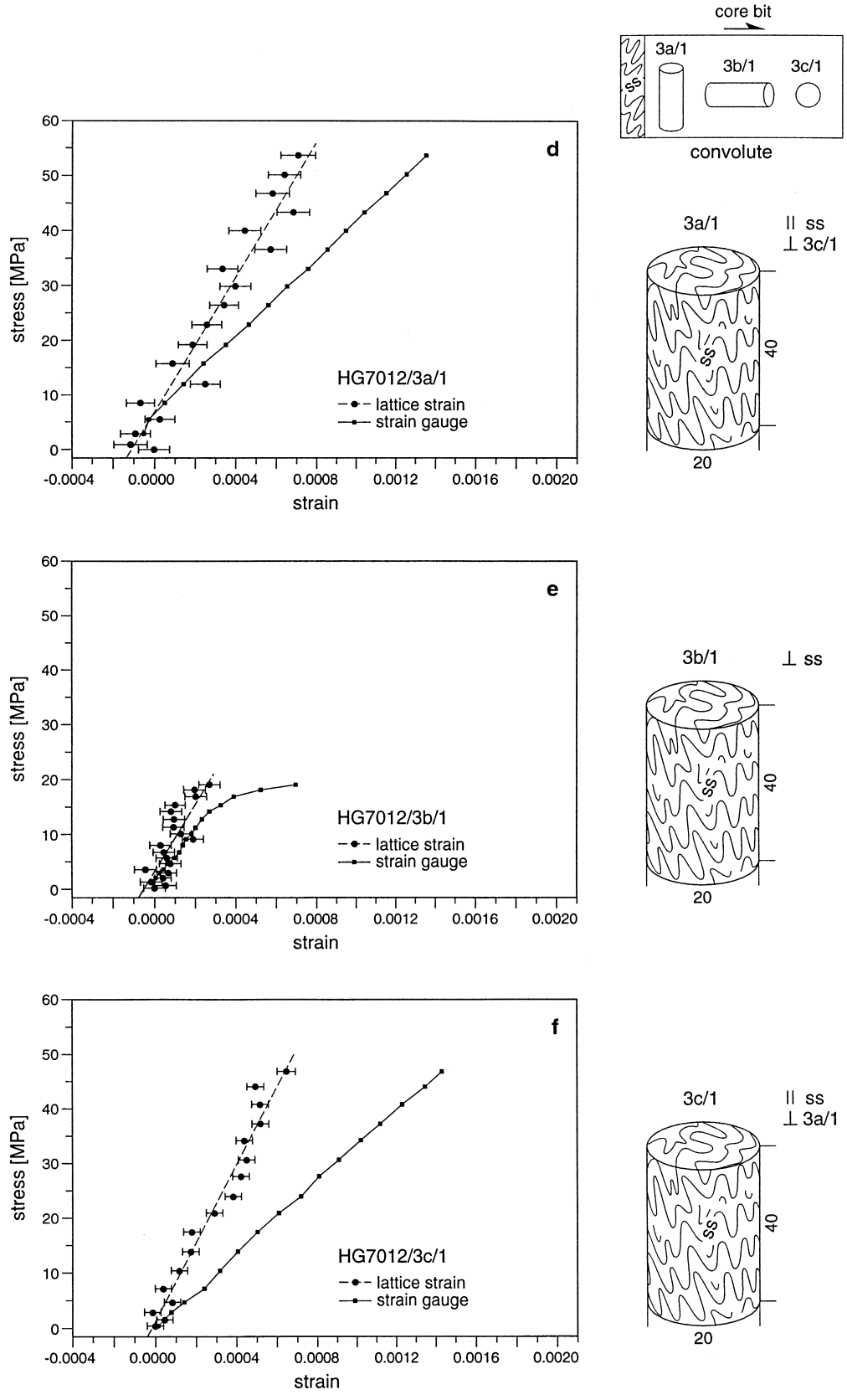

Fig. 13. *continued*.

Table 2
Calculated elastic stiffness for sandstone of different types of bedding (ss) under load

Elastic stiffness [GPa]	Specimen label					
	Laminate bedding			Convolute bedding		
	1b ⊥ ss	1c ∥ ss	1d ∥ ss	3b ⊥ ss	3a ∥ss	3c ∥ss
Crystallographical	84.6±4.0	90.4±9.4	85.4±5.3	61.9±11.0	62.1±4.3	70.8±3.6
Mechanical	32.6±0.7	29.0±0.9	25.6±0.4	44.2±1.8	35.2±0.3	33.0±0.3

will vanish. On the other hand, a scattering angle $2\vartheta > 90°$ will cause a non ideal gauge volume. The time error and the angle error are about 3×10^{-3} and are constant during the experiment; these errors contribute to the width of the diffraction peaks. The length error can influence the peak position, because different paths may occur. In the worst case, the absolute length error may be 1 cm and the relative length error will be 1×10^{-4}.

In the 'transmission' case, i.e. for strain measurement in the direction of the applied load, the flight path through the sample is constant and equals $d \times 2^{1/2}$ for the plane containing the sample axis where d is the thickness of the sample. Absorption and other attenuation of the beam cannot influence the position of the Bragg-peak. In the 'reflection' case, the path-difference through the sample varies from zero to $2d \times 2^{1/2}$ (this holds of course, only if no diaphragms limit the incident and the diffracted beam). Using diaphragms for the incident and the diffracted beam the difference of the path inside of the sample will be $4w$, where w is the width of the diaphragm slit. The difference can be as much as 2 cm.

Quartz has a small absorption cross-section, with a linear absorption coefficient of about 0.036 cm^{-1} for the $(10\bar{1}1)$-reflection. Due to the path difference inside the sample the loss of neutrons is about 7% for the maximal path length in comparison with the minimal one. The consequence of small absorption is that a neutron beam passing through an isotropic polycrystal will be attenuated mainly by scattering. In the case of quartz, the incoherent scattering length is small in comparison with the coherent one and therefore we consider only coherent scattering. For the $(10\bar{1}1)$-peak, we estimate the coherent scattering cross-section to be 2.7 barns and therefore the linear attenuation coefficient to be in the order of 1.7 cm^{-1}. This means that the shorter path is strongly favoured. The influence on peak position has to be investigated by further Monte-Carlo-calculations.

For cubic materials it is well known that lattice planes with variant hkl show different sensitivity or different response to an applied uniaxial load. This is expressed by the so called anisotropy factor A_{hkl} (Hutchings, 1992; Webster, 1992) which is a function of the Miller indices. This anisotropy should exist for other crystal symmetries too, but up to now only a few papers report this (e.g. Allen et al., 1985). Detailed investigation of the response of the variant planes on applied loads for lower crystal symmetry are required.

Our initial results on sandstones have indicated that neutron diffraction is a suitable tool for in situ and direct stress–strain investigations on geological materials. The results indicate a pronounced difference between macroscopic (sample) and microscopic (lattice) strain, caused by the combination of geological features of the sample, including the anisotropic effects of residual stress distribution and strain partitioning. It could be shown that only the macrostructural feature 'bedding' in sandstone alone (even under the conditions of absent crystallographic preferred orientation of quartz) has considerable influence on the stress–strain behaviour of rocks. Furthermore, anisotropic residual stress distribution combined with a depth dependent change from compressive to extensive conditions was observed by residual stress measurements within the bedding plane of laminated sandstone, orientated perpendicular to the axis of the cylinder sample.

The difference between lattice strain data and mechanically measured values reflects the influence of specific changes within the sample such as changes in the orientation of grains as well as the reconstruction of the pore volume or the anisotropy of the elastic constants within the involved crystals. The intensity of strain partitioning and the order of difference between crystallographically and mechanically determined data depends, for instance, on the type of bedding. As expected, a greater difference between crystallographically and mechanically determined data is observed for the samples with laminated bedding. In order to check the discrepancy of macro- and microstrain for rocks of different structural characteristics, additional investigations of the microstructural change after deformation are needed. A contribution to the discrepancy, although uncertain because the used quartz $(02\bar{2}1)$-reflection does not have the highest Young's modulus, arises from strain partitioning between grains with different crystallographic orientation. Thus, the peak shifts of several reflections must be measured and compared (TOF-method). However, due to the limited beam time the experiments using the monochromatic diffraction have been restricted to recording in one lattice plane only.

The studied samples may be considered as monomineralic, since they consist mainly of quartz. Future experiments with rocks composed of different phases (polymineralic samples) and/or geological specimens with other types of crystallographic preferred orientation would result

in much more pronounced stress–strain partitioning, as could be demonstrated here for two different types of bedding. Furthermore, if the method is extended to polyphase systems this can contribute to a better understanding of the processes of strain partitioning in rocks and its significance for deformation processes in rocks, because stress–strain states of individual components may be investigated separately, non destructively and simultaneously. Internal elastic strain created as a consequence of inhomogeneous plastic flow during loading of a polyphased material may produce strain incompatibilities in the sample which can result in tensile residual stress even under compressive macroscopic stress (Bourke et al., 1993).

The studied samples represent a low-level stress region of the crust in Middle Europe (Elbezone), situated on a consolidated crust but within the borders of a tectonically exposed structure which is characterized by slightly higher recent crustal activity in comparison to its adjacent regions. Particularly under those conditions, low-level anisotropic features related to strain partitioning and/or residual stress distributions may contribute to the stress behaviour of rocks if they are superimposed by a regional low-level recent stress field. Those low-level recent stress fields are typical for platforms. A stronger recent stress field will efface the effect of sample-inherent stress–strain features. There is no doubt that a more improved and extended data base, both from the physical and the geological point of view, are needed before the method may be used for regional geological assertions.

Acknowledgements

The project was supported by the German Ministry for Education, Science and Technology under the project number 03DUBPOT3, the Joint Institute for Nuclear Research Dubna (Russia), the Nuclear Physics Institute Řež (Czech Republic) and GeoForschungsZentrum Potsdam (Germany). The authors would like to thank Dr K. Bennett (Los Alamos National Laboratory) for helpful comments to an earlier draft and Dr P. Denny for improving the English.

References

Allen, A.J., Hutchings, M.T., Windsor, C.G., Andreani, C., 1985. Neutron diffraction methods for the study of residual stress fields. Advances in Physics 34, 445–473.

Amadei, B., Stephansson, O., 1997. Rock Stress and its Measurement. Chapman & Hall, London.

Bankwitz, P., Betzl, M., Drechsler, L.P., Feldmann, K., Fuentes, L., Kämpf, H., Walther, K., 1985. Fabric analysis of the quartz component in granulite rocks using neutron time-of-flight diffraction. Gerlands Beiträge Geophysik 94, 507–521.

Bourke, M.A.M., Goldstone, J.A., Stout, M.G., Lawson, A.C., Allison, J.E., 1993. Strain measurement in individual phases of an Al/Tic composite during mechanical loading. In: Barrera, E.V., Dutta, I. (Eds.), Residual Stresses in Composites. Measurement, Modeling and Effects on Thermo-Mechanical Behavior. The Minerals, Metals and Materials Society, pp. 67–77.

Eigenmann, B., Macherauch, E., 1995. Röntgenographische Untersuchung von Spannungszuständen in Werkstoffen. Materialwissenschaften und Werkstofftechnik 26, 148–160.

Friedman, M., 1972. Residual elastic strain in rocks. Tectonophysics 15, 297–330.

Hutchings, M.T., 1992. Neutron diffraction measurements of residual stress fields: Overview and points for discussion. In: Hutchings, M.T., Krawitz, A.D. (Eds.), Measurement of Residual and Applied Stress using Neutron Diffraction. Kluwer Academic Publishers, pp. 3–18.

Hsu, T.C., Marsiglio, F., Root, J.H., Holden, T.M., 1995. Effects of multiple scattering and wavelength-dependent attenuation on strain measurements by neutron scattering. Journal Neutron Research 3, 27–39.

Mikula, P, Vrána, M., Lukáš, P., Šaroun, J., Strunz, P., Ullrich, H.J., Wagner, V., 1997. Neutron diffractometer exploiting Bragg diffraction optics: A high resolution strain scanner. Abstract of proceedings of the 5th Int. Conf. on Residual Stresses (ICRS-5), Linkoping (Sweden).

Müller, B., Wächter, K., 1970. Beiträge zur Tektonik der Elbtalzone unter besonderer Berücksichtigung der Lausitzer Störung. Geodätisch Geophysikalische Veröffentlichungen Reihe III 18, 1–52.

Rauche, H., 1992. Spätvariszische Spannungs- und Verformungsgeschichte der Gesteine am Südwestrand der Elbezone (östliches Saxothuringikum, Varisziden). Dissertation, Ruhr-Universität Bochum.

Reik, G., 1976. Residuelle Spannungen in quarzreichen Gesteinen. Röntgendiffraktometrische Messung und Erklärungsmöglichkeiten ihrer Entstehung. Geologische Rundschau 65, 66–83.

Scheffzük, Ch., Frischbutter, A., Mikula, P., Vrána, M., 1998a. Double bent-crystal neutron diffractometer for quartz strain measurements on sandstones from the Elbezone. Schriftenreihe für Geowissenschaften 6, 9–18.

Scheffzük, Ch., Frischbutter, A., Walther, K., 1998b. Intracrystalline strain measurements with time-of-flight neutron diffraction: Application to a Cretaceous sandstone from the Elbezone (Germany). Schriftenreihe für Geowissenschaften 6, 39–48.

Sim, L.A., Korcemagin, V.A., Frischbutter, A., Bankwitz, P., 1999. The neotectonic stress field of the East European Platform. Zeitschrift für geologische Wissenschaften 27 (314), 161–181.

Thurm, H., Lang, A., Bankwitz, P., Manthey, W., 1968. Komplexe Untersuchung en rezenter Krustenbewegungen im Testgebiet Elbtalzone. Geodätisch Geophysikalische Veröffentlichungen Reihe III 11, 1–68.

Thurm, H., Bankwitz, P., Bankwitz, E., 1977. Rezente horizontale Deformation der Erdkruste im Südostteil der Deutschen Demokratischen Republik. Petermanns Geographische Mitteilungen 4, 281–304.

Voight, B., 1966. Interpretation of in-situ stress measurements. Panel Report on Theme IV, Proceedings of the 1st Congress of the International Society of Rock Mechanics (ISRM), Lisbon III, 332–348.

Vrána, M., Lukáš, P., Mikula, P., Kulda, J., 1994. Bragg diffraction optics in high resolution strain measurements. Nuclear Instruments and Methods A338, 125–131.

Walther, K., Frischbutter, A., Scheffzük, Ch., 1998. The Diffractometer Epsilon for the measurement of strains: An estimation of the full stress tensor, Schriftenreihe für Geowissenschaften 6, 19–28.

Webster, B., 1992. Role of neutron diffraction in engineering stress analysis. In: Hutchings, M.T., Krawitz, A.D. (Eds.), Measurement of Residual and Applied Stress using Neutron Diffraction. Kluwer Academic Publishers, pp. 51–65.

Wenk, H.-R., Kern, H., Wagner, T., 1981. Texture development in experimentally deformed limestone. Abstract of proceedings of the 2nd Risø International Symposium on Metallurgie and Material Sciences 235–244.

Wenk, H.-R., 1985. Preferred Orientation in Deformed Metals and Rocks An Introduction to Modern Texure Analysis. Orlando-Academic Press Inc, London.

Wieder, T., 1996. Simultaneous determination of the stress–strain tensor and the unstrained lattice constants by X-ray diffraction. Applied Physics Letters 69, 2495–2497.

Zoback, M.L., 1992. First- and second-order patterns in the lithosphere: The world stress map project. Journal Geophysical Research (B8), 97, 11703–11728.